Taylor & Francis
Taylor & Francis Group

MULTISCALE AGENT-BASED SIMULATION FOR CHONDROGENIC PATTERN FORMATION *IN VITRO*

SCOTT CHRISTLEY

Department of Computer Science and Engineering, and Interdisciplinary Center for the Study of Biocomplexity, University of Notre Dame, Notre Dame, Indiana, USA

XUELIAN ZHU

Department of Material Science and Engineering, University of Pennsylvania, Philadelphia, Pennsylvania, USA

STUART A. NEWMAN

Department of Cell Biology and Anatomy, New York Medical College, Valhalla, New York, USA

MARK S. ALBER

Department of Mathematics and Interdisciplinary Center for the Study of Biocomplexity, University of Notre Dame, Notre Dame, Indiana, USA

Mathematical and computational multiscale models are becoming increasingly important investigative tools in developmental biological research. During certain developmental processes cells that start out as independent entities interact to form multicellular structures.

Address correspondence to Mark Alber, Department of Mathematics and Interdisciplinary Center for the Study of Biocomplexity, University of Notre Dame, Notre Dame, Indiana 46556, USA. E-mail: malber@nd.edu

Cells of the embryonic vertebrate limb in high-density culture undergo chondrogenic pattern formation, which results in the formation of regularly-spaced "islands" of cartilage analogous to the cartilage primordia of the developing limb skeleton. In this article we describe a discrete, agent-based stochastic model for studying the behavior of limb bud precartilage mesenchymal cells *in vitro*. This model, like an earlier one, employs a biologically motivated reaction-diffusion process and cell-matrix adhesion as the basis of self-organizing pattern formation, but constitutes an improvement in biological fidelity over previous descriptions in that it is multiscale (i.e., cell and molecular dynamics occur on distinct scales), and the cells are represented as spatially extended objects. The improved model reproduces a broader set of results of the micromass culture system than the previous one and discloses multiple dynamical regimes that suggest new biological experiments.

INTRODUCTION

Mathematical and computational models have played an increasingly prominent role in developmental biology in recent years (Forgacs and Newman 2005). These models serve to provide tests of the plausibility and robustness of proposed mechanisms of morphogenesis and pattern formation. Equally importantly, they can suggest new hypotheses and previously unknown but experimentally testable consequences or hypotheses from known biological interactions.

Models of biological problems fall into two categories: continuous models that use families of differential or integro-differential equations to describe "fields" of interaction, and discrete models in which space, time or state may be discrete. Models may be deterministic or stochastic. In biological applications, continuous models have been used to describe oceanic microbial cycles (Belov and Giles 1997), microbial growth dynamics (Panikov 1995), the spread of species through an ecosystem (Scott et al. 1995), and biofilm formation (Wanner, 1996). Discrete models describe individual (microscopic) behaviors. They are often applied to microscale events where a small number of elements can have a large (and stochastic) impact on a system. Discrete methods that have been applied to biological systems include cellular automata (Ermentrout and Edelstein-Keshet 1993), lattice-gas-based cellular automata (Alber et al. 2004; Sozinova et al. 2005), the cellular Potts model (Glazier and Graner 1993), and agent-based modeling (Walker et al. 2004). The choice of discrete versus continuous models

depends upon the entities being represented and the level of detail desired for the interactions between the entities. Parunak et al. (1998), for example, discuss the criteria for using an agent-based versus an equation-based model in a case study of a manufacturing supply chain simulation; while Wilson (1998) contrasts the two types of models for predator-prey population dynamics.

The developing limbs, or limb buds, of embryos of vertebrate organisms such as chickens or mice, contain an interior population of loosely packed cells ("mesenchyme"), enclosed by a thin layer of embryonic skin, or ectoderm. The precartilage mesenchymal cells undergo a process of chondrogenic (i.e., cartilage) pattern formation whereby they first become more tightly packed at discrete sites, forming "condensations." These precartilage condensations then differentiate into nodules or bars of cartilage which form the primordia of the developing limb skeleton (reviewed in Newman 1988). When grown in high density ("micromass") culture, the same limb bud-derived cells undergo pattern formation that is similar in spatial scale and cellular and molecular mechanisms to that in the embryonic limb. Theoretical and experimental considerations suggest that in both cases an activator-inhibitor network of diffusible signal molecules ("morphogens") with formal attributes of the Turing instability (Turing 1952) are responsible for the basic patterning process (Newman and Frisch 1979; Miura and Shiota 2000a, b; Hentschel et al. 2004; Miura et al. 2006).

Here we describe a discrete, multiscale, agent-based stochastic model for studying behavior of these cultures which accurately simulates their formation of patterns of precartilage condensation. We present this model not only as an example of posthoc analysis of experimental findings, but also as a tool for experimental design and hypothesis testing. In particular, the cellular and molecular features we model (cell movement and shape change, cell-cell signaling, cell adhesion, among others) are found in a variety of *in vitro* systems derived from developmental and cancer cell biology. The plausibility and limitations of postulated interactions and mechanisms, for example, reaction-diffusion as the basis for mesenchymal pattern formation, can be judged in simulations with this model, the strength of which is the facility with which it can be revised based on new information and experimental outcome.

In the example presented here, calibration of certain key model parameters with experimentally determined values obtained in related or analogous systems leads to the emergence of condensations with

the same size and spatial distribution as those in cultures of limb bud precartilage mesenchymal cells. Our simulations have also disclosed two distinct regimes of dynamical behavior in the reaction-diffusion system that provide motivation for new biological experiments to explore the underlying molecular mechanisms.

The organization of the article is as follows. We initially provide some biological background regarding chondrogenic pattern formation to motivate the development of an agent-based model. Following that, we describe the computational details including the spatial, agent, and molecular representations, the algorithms and equations used to implement the model, and the scheduling and integration of all the components. Next, we calibrate the parameters of the model with known experimental values. Finally, we provide some simulation results and discuss their implications for the use of agent-based models for biological development. Additional results using the model are given in Christley et al. (2007).

BIOLOGICAL BACKGROUND

Skeletal pattern formation in the developing vertebrate limb depends on interactions of precartilage mesenchymal cells with factors that control the spatiotemporal differentiation of cartilage. The most basic skeletogenic processes involve the spatial separation of precartilage mesenchyme into chondrogenic and nonchondrogenic domains. *In vitro* as well as *in vivo*, TGF-βs and other members of this superfamily of morphogens induce precartilage condensation by a process that involves the upregulation of the secreted extracellular matrix protein, fibronectin. Mesenchymal cells accumulate at sites of fibronectin deposition due to increased cell-matrix adhesive interactions and then transiently adhere directly to one another by virtue of cell-cell adhesion molecules, the enhanced expression of which are also induced by TGF-β. Cartilage differentiation, or chondrogenesis, follows at the sites of condensation *in vitro* and *in vivo* (reviewed in Newman and Müller 2005).

Earlier work has suggested that interactions between diffusible activators and inhibitors of chondrogenesis can explain the approximately periodic patterns of chondrogenesis in the developing limb (Newman and Frisch 1979; Hentschel et al. 2004; Miura et al. 2006) and in micromass cultures (Miura and Shiota 2000a, b; Miura and Maini 2004; Kiskowski et al. 2004). In particular, the morphogen TGF-β acts as an activator of precartilage condensation by positively regulating its own production (Miura and Shiota 2000b), as well as that of fibronectin

(Leonard et al. 1991; Downie and Newman 1995). The nature of the lateral inhibitor of condensation is more elusive. Recent work suggests that it depends both on signaling via fibroblast growth factor receptor 2 (FGFR2) (Moftah et al. 2002) and the juxtacrine (cell-cell contact-activated) Notch receptor (Fujimaki et al. 2006), both of which appear on cells at sites of incipient condensation. Here we assume that the experimentally based lateral inhibitory effect is due to a diffusible morphogen, though other modes of propagation of an inhibitory signal are possible.

COMPUTATIONAL MODEL

In a previous study (Kiskowski et al. 2004), we presented a biological lattice gas model that remains the most successful computational model to date for pattern formation in the limb cell micromass system. The present model more closely reflects biological reality than the earlier one in several important respects. First, the cells in the new model are extended, multi-pixel objects that can change shape. Adjacent cells are separated by less than a cell diameter, condense without denuding the regions surrounding condensation centers, and are not irreversibly trapped once entering a condensation. Chemical reactions, molecular diffusion, and diffusion of cells operate on different physical and temporal scales. Finally, key simulation parameters are calibrated to corresponding physical measurements, where available, including the physical area of a cell, which is equal to the average surface area of a limb cell in the micromass.

Whereas the model of Kiskowski et al. (2004) was written in Matlab, the current model was ported from the original Matlab source to the C programming language for scalability and efficiency of execution, and then to the Objective-C programming language to take advantage of object-oriented features. We still use Matlab for visualizing data produced by simulation runs. The source code is available as free software from the authors.

In the following sections, we describe the details of our discrete, multi-scale agent-based stochastic computational model whereby the cells and molecules are represented as discrete agents that occupy spatial grids of differing resolution and interact according to a predefined set of rules.

Spatial Model

The spatial environment that cells and molecules occupy is modeled as a two-dimensional discrete grid. The implementation provides support for

multiple overlaid grids of various spatial scales. In our current model, we only employ two scales; one for the cellular level and another finer resolution scale for the molecular level. The coarsest resolution spatial scale (the cellular level for our model) is considered to be the base spatial scale, and all other grids are an integer ratio size of that base grid. A ratio size of two corresponds to four times the area resolution for a two-dimensional grid, so four pixels of the finer resolution grid, so that four pixels fit into one pixel of the base spatial grid. The base spatial grid can be defined as a square or rectangular grid of any height and width, and all of the grids overlay one another and cover the same physical area.

Our model supports both periodic and no-flux boundary conditions. With periodic boundary conditions, cells or molecules crossing a grid boundary will immediately appear on the opposite side of the grid, while with no-flux boundary conditions, the grid boundary acts as a barrier or obstacle that prevents cells and molecules from moving in that direction. No-flux boundary conditions can create situations whereby cells or molecules get stuck in corners or have less possibility of moving away from a boundary. We have not attempted to adjust this behavior at the boundary because such physical obstacles can accurately represent features of the physical domain, i.e., the edge of a cell-culture dish or the epithelial covering of a limb bud.

Agent-Based Cell Representation

Each cell is a discrete agent represented as a set of seven contiguous pixels operating on the base spatial grid as shown in Figure 1(a). We chose the simplest multipixel representation of limb mesenchymal cells subject to the following biological constraints: (i) cells have essentially isotropic geometry, that is they do not elongate in the direction of migration but rather probe their environment by extending short randomly oriented projections; (ii) the cell nucleus is also isotropic but is relatively unchanging in shape and comprises more than half the cell volume; (iii) cells in fibronectin-rich, condensing areas of the micromass round up such that their cross-section in the plane of the culture is significantly reduced (Cui 2005). We maintain four pixels in a two-by-two square (kernel) configuration that represents the portion of the cell that contains the nucleus and allow the remaining pixels to occupy the border region around the nucleus. Cells that round up shrink their spatial area to five pixels as shown in Figure 1(c), the lost pixels moving into a virtual third dimension.

Cell diffusion is implemented as a random walk (see Algorithm 1). If the cell moves, then all of its seven (or five) pixels move one pixel in a
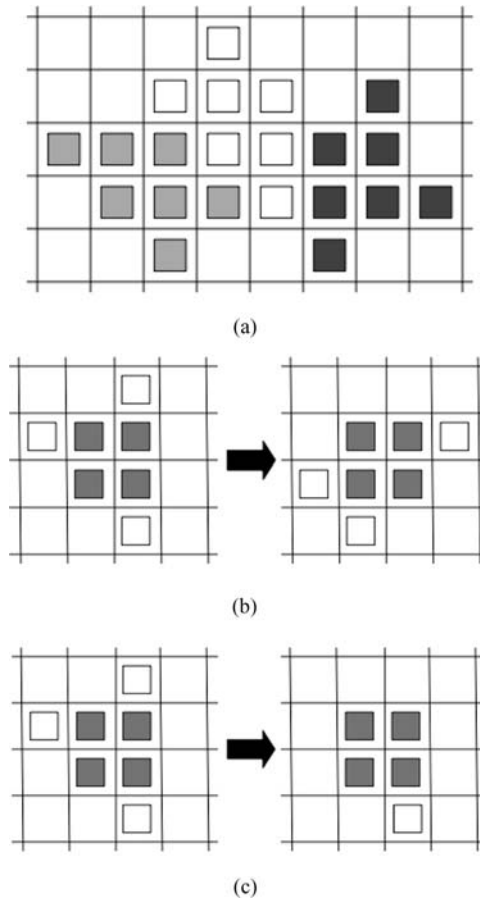
Figure 1. (a) Three cells on the spatial grid each occupying seven pixels. (b) Cell changes shape. The region of the cell that contains the nucleus, indicated by the four gray pixels, is structurally maintained; two border pixels move to new locations (one moving down and the other moving left), and one border pixel (upper right) displaces a nucleus pixel, by moving down while the nucleus pixel gets shifted to the right. (c) Cell rounding up on fibronectin. The surface area with fibronectin is reduced with two border pixels moving into a quasi third dimension above the cell.

given direction. Cells can also fluctuate in shape, yet such fluctuations maintain a structural representation of the nucleus by preserving intact a two-by-two square block of pixels (see Algorithm 2). Therefore, shape fluctuations are restricted to the motion of the three border pixels around the nucleus which either move to new positions on the border or displace

a nuclear pixel; Figure 1(b) gives examples of both types of fluctuations for a cell changing shape.

The rates and probability by which cells move and change shape are parameterized separately from movement of molecules so that they can be calibrated to the scale of actual biological cells. Unlike the representation of cells in the cellular Potts model (Glazier and Graner 1993; Chaturvedi et al. 2005; Merks and Glazier 2005), the properties of the cell are not described with energy expressions that are minimized as the simulation executes. Instead each cell is a discrete agent that behaves according to a predefined set of rules, and model parameters are used to adjust these rules.

Analysis of cell movement and shape within precartilage condensations (Cui 2005) indicates that cells have a smaller contact area with substratum close to the condensation center and that the rate of movement of those cells slightly but significantly increases. We model this behavior by shrinking the area of cells associated with levels of fibronectin above a threshold value from seven pixels to five pixels (see Figure 1(c)), and increasing the rate at which those cells can move and change shape. Likewise once a cell ventures onto a fibronectin-rich region, it has the tendency to remain there with a low probability of leaving the condensation.

Algorithm 1 moveWithProbability(p)
　　If random number $< p$ **then**
　　　　Randomly pick direction (up, down, left, right).
　　　　If movement does not overlap another cell **then**
　　　　　Move cell.
　　　　/* **Else: overlap so prevent move, cell maintains current position** */
　　　　End if
　　End if

Algorithm 2 changeShape()
　　If cell size is 7 pixels **then**
　　　　Randomly pick 3 border pixels.
　　Else /* cell size is 5 pixels */
　　　　Randomly pick 1 border pixel.
　　End if
　　If selected pixels do not overlap another cell **then**
　　　　Set new border pixels for cell.
　　/* **Else: overlap so prevent shape change, cell maintains current shape** */
　　End if

Molecular Model and Reaction-Diffusion Mechanism

The reaction-diffusion mechanism, introduced by Turing (1952) as a means for producing self-organizing spatial patterns, is based upon the interaction of slow diffusing, positive feedback activator molecules and fast diffusing, negative feedback inhibitor molecules. In our model, a discrete number of activator and inhibitor molecules occupy each pixel on the grid, and each molecule is considered to have a spatial extent of just one pixel. Each type of molecule has its own spatial grid independent of the other molecule types, so any number of molecule types can be defined, each with their own scale relative to the base spatial scale.

We model the reaction dynamics of the activator and inhibitor molecules at each pixel as follows: let U_t and V_t be the concentration of the activator and inhibitor, respectively, at time t and let ϕ_t be an indicator function for the existence of a cell at a pixel at time t.

$$\Delta U_t = \min\{MAX_U, (k_1 U_t + B_U)\phi_t + k_2 V_t\} \tag{1}$$

$$\Delta V_t = \min\{MAX_V, k_3 U_t \phi_t + k_4 V_t\} \tag{2}$$

Equation (1) shows the change over time for each pixel on the grid of the activator morphogen concentration based upon a proportion (as defined by chemical reaction rates) of the current activator and inhibitor concentrations. Equation (2) shows the corresponding change over time for each pixel on the grid for the inhibitor morphogen. The activator morphogen is considered to be a positively self-regulating molecule and a positive regulator of the inhibitor; thus, the chemical rate parameters k_1 and k_3 both have positive values. The inhibitor morphogen is considered a negative regulator of activator that decays over time; thus, the values of the chemical rate parameters k_2 and k_4 are both negative.

The change of activator and inhibitor morphogens is calculated for each pixel on the grid for each time step of the simulation, and the concentrations of the two morphogens are updated at each pixel.

$$U_{t+1} = \max\{0, U_t + round(\Delta U_t)\},$$

$$V_{t+1} = \max\{0, V_t + round(\Delta V_t)\}.$$

In keeping with the biology, we consider cells to respond to low concentrations of morphogens and therefore represent morphogen molecules as discrete entities. Consequently, the morphogen concentrations (U_t, V_t) are whole numbers, and changes in the concentrations at a time step

are rounded to the nearest integer and prevented from becoming negative. Nonetheless, we treat the chemical rate parameters (k_1, k_2, k_3, k_4) for the two morphogens as averages of the reaction rates and allow them to assume real number values.

In our model, production of the activator and inhibitor molecules, as represented by the k_1 and k_3 parameters, can only occur in the presence of a cell. In contrast, the decay of activator and inhibitor, as represented by the k_2 and k_4 parameters, are considered to occur independently of cell presence. Cells are initially randomly distributed on the grid, and secrete a small basal amount (B_U) of activator morphogen, which provides the initial concentration of activator; inhibitor concentration starts at zero.

In any physicochemical reaction, there are limitations on how much reagent a single cell can realistically produce during any period of time. For this reason, our model provides separate parameters (MAX_U, MAX_V) for the maximum amount of activator and inhibitor that can be produced during a single reaction step. The maxima are imposed on individual pixels of the molecular grid rather than across the entire cell to reflect the polarization of limb mesenchymal cells (Holmes and Trelstad 1980). This allows for small morphogen gradients to be present across the spatial extent of an individual cell through spatially polarized secretion of morphogens. The peaks of activator concentration produced by the reaction-diffusion dynamics define a large prepattern equal in spatial area to the fibronectin-rich patches, containing around fifty cells within a single patch, so polarization plays a role for the cells on the border region of the patch; while cells in the patch interior perceive a relatively constant morphogen concentration across their entire spatial extent.

Molecular diffusion from any pixel can occur randomly toward any of the four neighboring pixels (up, down, left, right). The diffusion rate (D_U, D_V) is scaled into a probability factor $0 < p < 1$ and a time step n such that $D = pn$. The probability determines the chance that a molecule will diffuse, and the time step indicates how many opportunities a molecule has to diffuse for a single simulation iteration. If the molecule diffuses, then one of the four neighboring pixels is picked with equal probability. The chemical reaction operates at a much slower rate than molecular diffusion, so the time scales are separated, with diffusion calculated at a small time step and the reaction calculated at a longer time step. Algorithm 3 shows how the diffusion is performed at a finer time scale.

Algorithm 3 calculateReactionDiffusion()
    Calculate chemical reaction for each pixel on grid.
    For $i = 1$ to n **do**
        Calculate activator and inhibitor diffusion for each pixel on grid.
    End for

Fibronectin Production

Fibronectin is a nondiffusing, extracellular matrix molecule whose spatial distribution forms the template for precartilage condensations. As the concentration levels of the activator morphogen increase in the presence of a cell, that cell produces fibronectin mRNA which can then be translated into fibronectin protein molecules and secreted. We implement a simple threshold-sensing mechanism such that once the activator concentration exceeds the threshold value in the spatial presence of a cell, the cell differentiates into a fibronectin-producing cell. We separate the trigger for cell differentiation from the actual production of fibronectin by the cell to emulate delays seen in experiments.

When a cell produces fibronectin, a single multimolecular unit is secreted with random probability for each of the pixels on the molecular grid occupied by the cell, and each molecule is allowed to perform an initial small diffusion of at most one pixel (Kiskowski et al. 2004). Production of fibronectin molecules continues until a maximum concentration level is reached at a pixel, although cells may still continue to produce fibronectin on pixels that have not yet reach the maximum. The production rate of fibronectin, the duration of such production, and the maximum amount of fibronectin allowed per pixel, can be adjusted with model parameters.

Main Simulation

All of the various pieces including the cellular dynamics, the molecular dynamics, and fibronectin production can be brought together into the complete simulation code as shown in Algorithm 4. The scheduling of cell actions like movement and shape change is performed in an asynchronous manner and in random agent order. Molecular diffusion and chemical reaction is performed in a synchronous manner for the complete molecular grid. This is done in the normal way by utilizing a temporary matrix for holding the intermediate calculations, then that

temporary matrix is copied to the molecular grid thus updating the whole grid in one step. Fibronectin production can be performed either asynchronously or synchronously because the calculation is not dependent upon neighboring cell states, so we perform the calculation synchronously, which is slightly more efficient.

MODEL CALIBRATION

In attempting to calibrate our model parameters with known empirical parameters our objective is to correlate the *in silico* spatial and temporal patterns with *in vitro* experiments. For spatial patterns, we consider the size, shape, and distribution of the fibronectin-rich spatial domains. For temporal patterns, we consider the reaction rates of activator and inhibitor production, the diffusion rates of both cells and molecules, the onset of fibronectin production, the production rate of fibronectin, and the fluctuations of shape and movement of cells on fibronectin. The actual value for the set of key parameters used in the simulation and their corresponding physical measurements, if known, are shown in Table 1.

Diffusion Rates

Diffusion rates for the activator and inhibitor play a vital role in defining the wavelength of the Turing patterns produced by the reaction-diffusion dynamics that ultimately determine the size and distribution of the fibronectin-rich patches. Lander and coworkers calculate that the effective diffusion coefficient for a molecule the size and shape of the

---

Algorithm 4 Main Simulation
   For each simulation iteration **do**
      Generate randomized list, *R*, of agents
      For each agent in *R* **do**
         moveWithProbability(*p*)
         changeShape()
      End for
      calculateReactionDiffusion()
      Determine if any cells have reached threshold for differentiation.
      Calculate fibronectin production for each differentiated cell.
   End for

Table 1. Calibrated simulation parameters to known physical values

Parameter	Physical value	Simulation value
Cell diameter/area	$15\,\mu m / 177\,\mu m^2$	7 pixels
Cell spatial grid	$1.4 \times 1.0\,mm$	280×200 pixels
Molecular spatial grid		560×400 pixels
Spatial ratio cells:molecules	10000:1	28 pixels:1 pixel
Simulation Temporal scale	17.07 sec	1 iteration
Reaction Temporal scale	17.07 sec	1 reaction
Diffusion Temporal scale ($n = 200$)	85.3 msec	1 diffusion step
Basal activator production (B_U)	Unknown	28
Activator self-regulation (k_1)	Unknown	0.3356
Activator regulation of inhibitor k_3	Unknown	0.16
Inhibitor regulation of activator k_2	Unknown	-1.1
Inhibitor decay (k_4)	Unknown	-0.4615
Maximum activator produced (MAX_U)	Unknown	8000
Maximum inhibitor produced (MAX_V)	Unknown	8000
Activator diffusion rate (D_U)	$10\,\mu m^2 / sec$	27 pixels/iteration
Inhibitor diffusion rate (D_V)	Unknown	108 pixels/iteration
Cell diffusion rate	$0.42\,\mu m^2 / min$	1 pixel/60 iterations
Cell diffusion rate on fibronectin	$0.62\,\mu m^2 / min$	1 pixel/40 iterations

morphogen Decapentaplegic (Dpp) to be $10\,\mu m^2/sec$ (Lander et al. 2002). Since TGF-β, which we assume to be our activator morphogen based upon cell-culture experiments (Leonard et al. 1991; Miura and Shiota 2000b), is a morphogen of the same molecular class as Dpp, we take the diffusion coefficient of Dpp to be our activator diffusion rate. The inhibitor morphogen, whose identity is unknown, must spread at a faster rate than the activator morphogen for patterns to be produced. We have found that an inhibitor diffusion rate approximately four times faster than that of the activator is sufficient to produce stable patterns.

The diffusion rate for cells is considerably slower than for the activator and inhibitor molecules. Cui (2005) used phase-contrast microscopy and video-based cell tracking to measure the movements of cells during development of chicken limb precartilage mesenchyme over the time period of condensation formation. He determined an average cell diffusion coefficient of $0.506\,\mu m^2/min$, and his data are consistent with cells moving slightly faster in condensations (see also Ede et al. 1977). We implement this in a qualitative fashion by making cells associated with fibronectin diffuse faster than cells not associated with fibronectin (see Table 1).

Reaction Rates

Parameters for the reaction rates must fall within an appropriate "morphogenetic" region of parameter space in order for Turing-type patterns to be produced. Within this morphogenetic region, two types of behavior are observed for the morphogen concentrations: steady-state equilibrium with stable patterns and oscillatory behavior with transient patterns. The oscillatory behavior was induced by imposing the maxima (MAX_U, MAX_V) on production. Otherwise a steady-state would be attained, but at an unrealistically high concentration level of activator. As these reaction rates are unknown, we take the approach of choosing parameters that correspond to our understanding of the qualitative behavior of cells in culture.

Onset and Rate of Fibronectin Production

It was previously shown that brief, transient exposure of precartilage mesenchymal cells to exogenous TGF-β early in the culture period is sufficient to induce the production of precocious condensations a day later (Leonard et al. 1991). The cells responded to TGF-β by immediately producing elevated levels of fibronectin mRNA even though secretion of the fibronectin protein molecule in the discrete condensation pattern did not occur until the next day. In another study, the expression of FGFR2 protein (the mediator of FGF induction of the inhibitor at sites of incipient condensation) was found to be transient: it was no longer detectable once actual condensation was underway (Moftah et al. 2002). These results suggest that the signaling system that induces the spatiotemporal pattern of condensation (i.e., the reaction-diffusion mechanism under our hypothesis) does not have to maintain stable peaks of activation throughout the entire period of precartilage condensation. A set of transiently formed peaks could provide a prepattern for condensations occurring at a later time. Based upon these empirical observations, we selected reaction parameters in our model giving oscillatory behavior in order to test the idea that transient signaling could lead to subsequent condensation-like patterns.

The physical area of a biological cell determines the area of a pixel on the grid. This value, along with the assumed activator morphogen diffusion rate, permits the temporal scale of the morphogen diffusion, the chemical reaction, and the overall simulation to be calculated (cell

area $\times$ spatial ratio of cells to molecules $\times$ activator diffusion rate $=$ $\frac{177\,\mu m^2}{7\,\text{cell pixels}} \times \frac{1\,\text{cell pixel}}{4\,\text{molecular pixels}} \times \frac{27\,\text{molecular pixels·sec}}{10\,\mu m^2 \cdot \text{iteration}} = 17.07\,\text{sec/iteration}$).   The chemical reaction occurs on the same time scale as the overall simulation, but due to the separation of time scales diffusion occurs faster at $17.07\,\text{sec} \div 200 = 85.3\,\text{msec}$ for each diffusion step. Since *in vitro* experiments have not provided definitive values for the time course of morphogen activities, and the various morphogens may have other roles beyond induction of fibronectin production, we did not attempt to calibrate the duration of morphogen activity in our simulation to any known quantities. Instead, given the knowledge that cells respond quickly to TGF-β, we triggered cell differentiation early in our simulation, when the sum of units of activator across an entire cell reached a threshold value of 7,000. However, the transient signal of the morphogen concentrations occurs over a period of 500 simulation iterations which corresponds to a little over 2 h. While this appears to be somewhat faster than the corresponding change *in vitro*, it is well within an acceptable range that could be fine tuned once more is known about timing of events in the micromass culture system.

RESULTS

A comparison of *in vitro* and *in silico* results are shown in Figure 2. Visual inspection of the condensation patterns, as well as statistical analysis of five simulations with different random initial conditions (not shown), show a good match between the condensation patterns in a portion of a micromass culture (see Kiskowski et al. 2004, for details) and the typical output for the distribution of model cells in a simulation run with parameter choices as indicated in Table 1.

Given the set of parameter values that produces the condensation patterns, we explored nearby parameter space by varying key parameters by $\pm 5\%$ and running three replicate simulations for each of these modified systems. For a decrease of 5% in the activator self-regulation (k_1) smaller fibronectin patches were produced, with the patches spaced further apart from one another. Similar results were also obtained if the activator regulation of inhibitor (k_3) was increased by 5%. For a 5% increase in the activator self-regulation (k_1) fibronectin patches greatly expanded in size such that the patches touched one another, producing a pattern of interconnected stripes instead of spots. Similar results were obtained if the activator regulation of inhibitor (k_3) was
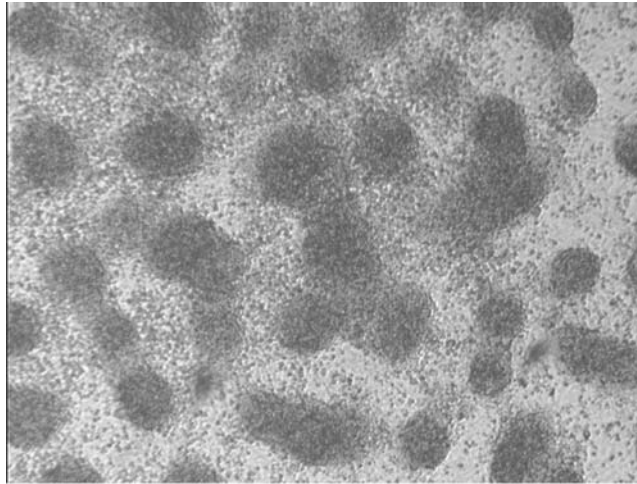
(a)
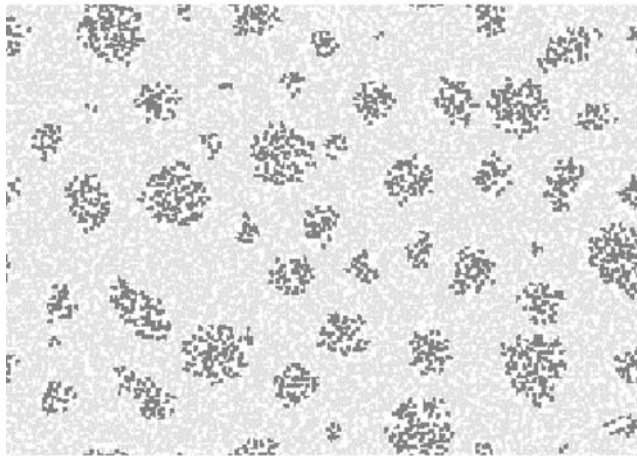
(b)

Figure 2. (a) Discrete spot-like precartilage condensations that have formed after 72 hours in a micromass culture of 5-day leg bud apical zone limb mesenchymal cells, visualized by Hoffman Contrast Modulation optics. Actual size of the microscopic field is 1×1.4 mm, and each condensation contains approximately 30–50 tightly packed cells. **(b)** Spatial grid of equal physical size as (a) containing over 6000 cells produced by simulation using the parameter values in Table 1 showing fibronectin-producing differentiated cells (dark gray), non-differentiated cells (light gray), and empty space between cells (white). Each cluster contains on average $\sim$30 cells. The fibronectin patches (not shown) are slightly larger than the clusters of differentiated cells, corresponding in size, shape, and distribution to the precartilage condensations in the micromass.

decreased by 5%. Changing the inhibitor regulation of activator (k_2) by either $+5$ or -5% did not significantly alter the size, shape or distribution of the fibronectin patches. Instead, the temporal dynamics were modified, causing an increase and decrease in the period of the morphogen oscillations with the $+5$ or -5% changes, respectively.

DISCUSSION

A benefit of the agent-based approach to cell culture simulation described here is the ease with which the contribution to biological phenomena of specific experimentally determined details can be evaluated as to their sufficiency and necessity. Furthermore, because very simple agent-based models can often capture "biological" features (Wolfram 2002), it is also useful to determine if basic models retain such behaviors when they are made more realistic.

In the case studied here, *in vitro* pattern formation in limb bud precartilage mesenchyme, the starting point was a simple agent-based model consisting of single-pixel agents representing biological cells, morphogens, and secreted macromolecular matrices on one uniform grid (Kiskowski et al. 2004), which captured many quantitative aspects of the pattern formation process. Our enhanced model incorporates multipixel cells with variable geometry and separation of spatial scales in the form of modeling cells and morphogen and extracellular matrix molecules on grids of differing mesh size. Realistic values of morphogen and cell diffusion have also been introduced.

These experimentally motivated modifications and constraints yielded a model that continues to generate, in a robust fashion, realistic patterns of cell condensation. In particular, the more sophisticated model produces fibronectin-rich patches corresponding to condensations in micromass cultures in size, shape, cell number, and spatial distribution. In contrast to the earlier model, but in keeping with biological findings, coverage of the virtual culture surface remained continuous as cells moved small distances, changed their shape in response to the deposited fibronectin matrix, and maintained their movement within, and capacity to leave, condensations once these had formed.

We initially separated the spatial scales in our desire for greater biological fidelity. However, we discovered that the multiple spatial scales required the introduction of multiple temporal scales, specifically between the morphogen diffusion and morphogen chemical reaction

but also with cell diffusion, in order for the parameters to be within the proper range for production of condensations of the appropriate size and distribution. Without the separation of time scales, the chemical reaction parameters would have to be scaled down to the morphogen diffusion time scale thus resulting in calculations which would be too imprecise due to rounding errors for low concentrations. Interestingly, if we performed the separation of time scales first, it would have likely led us to separating the spatial scales nonetheless because the cellular grid is too coarse for accurate simulation of our calibrated value for molecular diffusion. Our model provides a case study for how calibration to known experimental values may require introduction of multiple scales in order to provide simulation accuracy.

The match between the experimentally determined diffusion coefficient of an activator morphogen of the same molecular family as the one in our model and the model value required to produce condensations of the appropriate size and distribution suggests that our model is physically and biologically reasonable. Since the computational model provides fine control over the specification of how cells respond to morphogen concentrations and thus alter their functional and differentiated states, how they produce and secrete morphogens and extracellular matrix molecules (i.e., fibronectin), how they behave on extracellular matrices by, for example, changing their shape and motility, there is ample opportunity to introduce new experimental data. Experimental values of measured parameters provide constraints on unknown values which can be evaluated computationally and experimentally.

The dynamics of the model's cellular-biochemical network that emerge from simulations also suggest further experimental tests. An example is the discovery of stationary and oscillatory dynamical regimes that can both lead to pattern formation. Measuring TGF-β or fibronectin gene expression during different phases of the culture period can test the validity of the model, and most importantly, the model's predictions can be used to help determine the critical period for pattern formation.

Agent-based representations of developmental and other cellular systems afford a convenient way of moving between simulation and experiment. The model described here can provide a general framework for an interdisciplinary approach to studying cells in culture. The strategy can take the form of the following investigative cycle: (i) establishing a "core" biological model involving various simplifications and assumptions; (ii) computational implementation and calibration; (iii) comparison

of *in silico* experiments with *in vitro* biological experiments; (iv) suggestions for new biological experiments based on disparities between *in silico* and *in vitro* results; (v) new biological experiments and biological model improvement and/or revision of the computational model.

REFERENCES

Alber, M., Kiskowski, M., Jiang, Y., and Newman, S. 2004. Biological lattice gas models. In *Dynamics and bifurcation of patterns in dissipative systems*, edited by G. Dangelmayr and I. Oprea. Singapore: World Scientific, pp. 274–291.

Belov, A. P. and Giles, J. D. 1997. Dynamical model of buoyant cyanobacteria. *Hydrobiologia* 349: 87–97.

Chaturvedi, R., Huang, C., Kazmierczak, B., Schneider, T., Izaguirre, J. A., Glimm, T., Hentschel, H. G. E., Glazier, J. A., Newman, S. A., and Alber, M. 2005. On multiscale approaches to three-dimensional modeling of morphogenesis. *Journal of Royal Society (Lond.) Interface* 2: 237–253.

Christley, S., Alber, M. S., and Newman, S. A. 2007. Patterns of mesenchymal condensation in a multiscale, discrete stochastic model. *PL. S Computational Biology* 3: e77, 0743–0753.

Cui, C. 2005. Dynamics of cell movement and tissue motion in gastrulation and micromass cell culture. Ph.D. thesis, Indiana University.

Downie, S. A. and Newman, S. A. 1995. Different roles for fibronectin in the generation of fore and hind limb precartilage condensations. *Dev Biol* 172: 519–530.

Ede, D. A., Flint, O. P., Wilby, O. K., and Colquhoun, P. 1977. The development of precartilage condensations in limb bud mesenchyme *in vivo* and *in vitro*. In *Vertebrate limb and somite morphogenesis*, edited by D.A. Ede, J.R. Hinchliffe, and M. Balls. Cambridge: Cambridge University Press, pp. 161–179.

Ermentrout, G. B. and Edelstein-Keshet, L. 1993. Cellular automata approaches to biological modeling. *J Theor Biol* 160: 97–133.

Forgacs, G. and Newman, S. A. 2005. *Biological physics of the developing embryo*. Cambridge: Cambridge University Press.

Fujimaki, R., Toyama, Y., Hozumi, N., and Tezuka, K. 2006. Involvement of notch signaling in initiation of prechondrogenic condensation and nodule formation in limb bud micromass cultures. *J Bone Miner Metab* 24: 191–198.

Glazier, J. A. and Graner, F. 1993. A simulation of the differential adhesion driven rearrangement of biological cells. *Physical Review Part E* 47: 2128–2154.

Hentschel, H. G., Glimm, T., Glazier, J. A., and Newman, S. A. 2004. Dynamical mechanisms for skeletal pattern formation in the vertebrate limb. *Proc R Soc Lond B Biol Sci* 271: 1713–1722.

Holmes, L. B. and Trelstad, R. L. 1980. Cell polarity in precartilage mouse limb mesenchyme cells. *Dev Biol* 78: 511–520.

Kiskowski, M. A., Alber, M. S., Thomas, G. L., Glazier, J. A., Bronstein, N. B., Pu, J., and Newman, S. A. 2004. Interplay between activator-inhibitor coupling and cell-matrix adhesion in a cellular automaton model for chondrogenic patterning. *Dev Biol* 271: 372–387.

Lander, A. D., Nie, Q., and Wan, F. Y. 2002. Do morphogen gradients arise by diffusion? *Dev Cell* 2: 785–96.

Leonard, C. M., Fuld, H. M., Frenz, D. A., Downie, S. A., Massague, J., and Newman, S. A. 1991. Role of transforming growth factor-β in chondrogenic pattern formation in the embryonic limb: Stimulation of mesenchymal condensation and fibronectin gene expression by exogenous TGF-β and evidence for endogenous TGF-β-like activity. *Dev. Biol* 145: 99–109.

Merks, R. M. H. and Glazier, J. A. 2005. A cell-centered approach to developmental biology. *Physica A* 352: 113–130.

Miura, T. and Maini, P. K. 2004. Speed of pattern appearance in reaction-diffusion models: Implications in the pattern formation of limb bud mesenchyme cells. *Bull Math Biol* 66: 627–649.

Miura, T. and Shiota, K. 2000a. Extracellular matrix environment influences chondrogenic pattern formation in limb bud micromass culture: Experimental verification of theoretical models. *Anat Rec* 258: 100–107.

Miura, T. and Shiota, K. 2000b. TGFβ2 acts as an "activator" molecule in reaction-diffusion model and is involved in cell sorting phenomenon in mouse limb micromass culture. *Dev Dyn* 217: 241–249.

Miura, T., Shiota, K., Morriss-Kay, G., and Maini, P. K. 2006. Mixed-mode pattern in *Doublefoot* mutant mouse limb—Turing reaction-diffusion model on a growing domain during limb development. *J Theor Biol* 240: 562–573.

Moftah, M. Z., Downie, S. A., Bronstein, N. B., Mezentseva, N., Pu, J., Maher, P. A., and Newman, S. A. 2002. Ectodermal FGFs induce perinodular inhibition of limb chondrogenesis *in vitro* and *in vivo* via FGF receptor 2. *Dev Biol* 249: 270–282.

Newman, S. A. 1988. Lineage and pattern in the developing vertebrate limb. *Trends Genet* 4: 329–332.

Newman, S. A. and Frisch, H. L. 1979. Dynamics of skeletal pattern formation in developing chick limb. *Science* 205(4407): 662–668.

Newman, S. A. and Müller, G. B. 2005. Origination and innovation in the vertebrate limb skeleton: An epigenetic perspective. *J Exp Zoolog B Mol Dev Evol* 304: 593–609.

Panikov, N. S. 1995. *Microbial growth kinetics*. Berlin: Springer.

Parunak, H. V. D., Savit, R., and Riolo, R. L. 1998. Agent-based modeling versus equation-based modeling: A case study and users' guide. In: *Proceedings of the 1st workshop on modeling agent-based systems, MABS'98*, edited by

J.S. Schiman, R. Conte, and N. Gilbert. Lecture Notes in Artificial Intelligence, *Vol. LNAI 1534*, Berlin: Springer.

Scott, E. M., Rattray, E. A. S., Prosser, J. I., Killham, K., Glover, L. A., Lynch, J. M., and Bazin, M. J. 1995. A mathematical model for dispersal of bacterial inoculants colonizing the wheat rhizosphere. *Soil Biology and Biochemistry* 27: 1307–1318.

Sozinova, O., Jiang, Y., Kaiser, D., and Alber, M. 2005. A three-dimensional model of myxobacterial aggregation by contact-mediated interactions. *Proc Natl Acad Sci USA* 102: 11308–11312.

Turing, A. 1952. The chemical basis of morphogenesis. *Phil Trans Roy Soc. Lond B* 237: 37–72.

Walker, D. C., Hill, G., Wood, S. M., Smallwood, R. H., and Southgate, J. 2004. Agent-based computational modeling of wounded epithelial cell monolayers. *IEEE Transactions on Nanobioscience* 3: 153–163.

Wanner, O. 1996. Modelling of biofilms. *Biofouling* 10: 31–41.

Wilson, W. G. 1998. Resolving discrepancies between deterministic population models and individual-based simulations. *American Naturalist* 151: 116–134.

Wolfram, S. 2002. *A new kind of science.* Champaign, IL: Wolfram Media.